

Multilayer ion trap technology for scalable quantum computing and quantum simulation

A. Bautista-Salvador^{1,2,3}, G. Zarantonello^{1,2}, H. Hahn^{1,2}, A. Preciado-Grijalva¹, J. Morgner^{1,2}, M. Wahnschaffe^{1,2,3}, C. Ospelkaus^{1,2,3}

¹ Physikalisch-Technische Bundesanstalt, Bundesallee 100, 38116 Braunschweig, Germany

² Institute of Quantum Optics, Leibniz Universität Hannover, Welfengarten 1, 30167 Hannover, Germany

³ Laboratory for Nano- and Quantum Engineering, Leibniz Universität Hannover, Schneiderberg 39, 30167 Hannover, Germany

E-mail: amado.bautista@ptb.de

6 December 2018

Abstract. We present a novel ion trap fabrication method enabling the realization of multilayer ion traps scalable to an in principle arbitrary number of metal-dielectric levels. We benchmark our method by fabricating a multilayer ion trap with integrated three-dimensional microwave circuitry. We demonstrate ion trapping and microwave control of the hyperfine states of a laser cooled ${}^9\text{Be}^+$ ion held at a distance of $35\ \mu\text{m}$ above the trap surface. This method can be used to implement large-scale ion trap arrays for scalable quantum information processing and quantum simulation.

1. Introduction

Trapped ions are not only one of the most promising platforms for the practical implementation of quantum computing and quantum simulations, but also sensitive systems for measuring very small magnetic and electric fields. Typically, they are held in Paul or Penning traps at high vacuum, laser cooled close to absolute zero temperature, and their internal states coupled to their motion can be manipulated with high fidelity by either laser fields [1, 2] or microwave radiation [3, 4]. However, scaling these elementary demonstrations to larger systems remains a formidable technological challenge [5].

Surface-electrode ion traps [6] represent a strong candidate for the realization of a quantum charge-coupled device (QCCD) [7, 8] for scaling quantum logic operations. Such an ion trap array could feature dedicated zones for storing, manipulation and read-out, thus promising a modular hardware for quantum computation and quantum simulation [9]. Conventionally, in surface-electrode ion traps all electrodes are built in a single plane by standard microfabrication techniques [10]. First

integration of key scalable elements into a single layer chip such as micro-optical components [11], nanophotonic waveguide devices [12] or microwave conductors [13] have been demonstrated. However, interconnecting separated components built in this system imposes new challenges on trap design where signal lines have to be routed around other elements. Therefore, the realization of a highly integrated large-scale ion trap device requires a more flexible approach where signal routings can be distributed on vertically well-separated levels of interconnects.

Demonstrations of multilayer processes in ion traps so far are based on techniques borrowed from MicroElectroMechanical Systems (MEMS) [14, 15] or CMOS [16, 17]; however the resulting trap structures are limited to thin interconnect levels. Moreover, there is a need of a nearly material-independent processing capable of including most dielectric substrates and thick metallization. Any fabrication process will have to comply with the specific requirements of an ion trap, such as a material mix which features extremely low material outgassing and needs to be compatible with ultra-high vacuum (UHV) operation, low dielectric losses and non-magnetic metal surfaces. Often one is concerned about shielding the ion(s) from patch potentials due to exposed dielectrics. Specially, for the top-level the electrode interspacings should have at least a width equal to its height [18], or in other words electrode gaps of an aspect ratio higher than 1:1.

Here we present a robust fabrication method, scalable to an in principle arbitrary number of planarized thick metal-dielectric layers, enabling the realization of scalable ion trap devices. The method complies with the stringent requirements of a scalable ion trapping array, allowing the fabrication of complex trap designs using relatively forgiving fabrication techniques on nearly any type of substrate. To demonstrate the approach, we fabricate and operate a multilayer ion trap chip with three-dimensional (3-D) microwave circuitry towards the realization of high fidelity multi-qubit gates [13, 19].

2. Fabrication Methods

Methods for building surface-electrode ion traps [6] or atom chips [20, 21] are typically based on standard semiconductor processing. For the simplest case, in which all metal electrodes are aligned in a single plane, a generic fabrication workflow consists of a three-step processing: wafer patterning, electrode formation and electric insulation. Depending on the requirements one will choose between different materials and processing methods at hand. In what follows we will describe our own fabrication methods to build single layer and multilayer microfabricated ion traps.

2.1. Single Level Processing (SLP) Method

For the Single Level Processing (SLP) method all steps are carried out on 3-inch-diameter wafers in a fabrication line located at Physikalisch-Technische Bundesanstalt (PTB), Braunschweig. We have fabricated similar structures to the ones presented in Fig. 1 on AlN, sapphire, organic polymers and high resistivity (HiR) float zone (FZ) Si

wafers, demonstrating the compatibility of the method with a wide range of substrates suitable for ion trap technology.

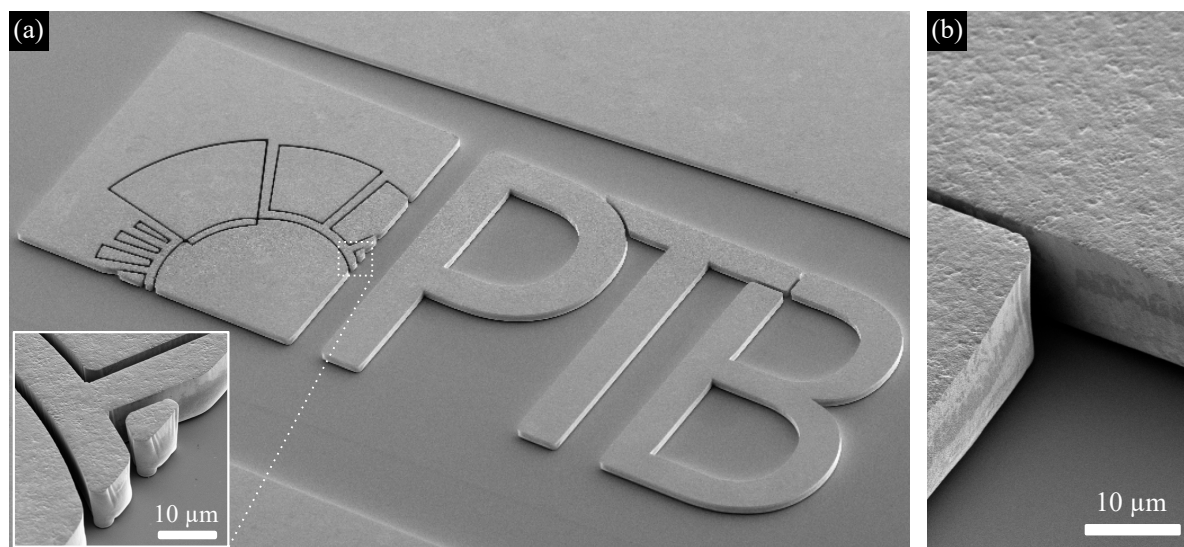


Figure 1. Gold structures with high aspect ratio supported on sapphire. (a) Au structures separated by gaps of about $2\ \mu\text{m}$ with a high aspect ratio of 5:1 (inset). (b) Pair of Au electrodes separated by a $0.8\ \mu\text{m}$ gap, resulting in a gap with an aspect ratio of 14:1. For both SEM micrographs shown in (a) and (b) the sample is tilted by 45° .

The first step during wafer preparation involves the deposition of a Ti adhesion layer (15 nm thin) and an Au seed layer (50 nm thin) on top of the substrate by resistive evaporation. The first film acts as an adhesion promoter between the substrate and the Au seed layer, and the second film serves as a starting conductive layer for a later electrodeposition step.

Second, to define the trap geometry, a 25- μm -thick positive or 16- μm -thick negative resist is spin coated on top of the Au seed layer and the wafer is exposed to UV light by contact lithography. A subsequent development of the exposed resist results in open areas on the substrate which are filled to a desired thickness by electrodeposition of Au in a sulphite-based bath.

Finally, after gold electroplating the resist mask is removed chemically and the wafer is cleaned under oxygen-based plasma etching. Additionally, the wafer is exposed to a fluorine-based plasma to further remove possible resist debris. Immediately afterwards the seed Au layer is removed via Ar etching and the Ti layer removed by a fluorine-based plasma etching.

This method allows the fabrication of gold structures with high aspect ratios as exemplified in Fig 1. Gold structures with a width as narrow as $5\ \mu\text{m}$ and gap separation as narrow as $2\ \mu\text{m}$ are shown in Fig. 1(a). Another example is depicted in Fig. 1(b) consisting of a pair of gold electrodes separated by a gap with an aspect ratio of 14:1. One additional advantage of the method is that after dry etching of the Au/Ti bilayer the resulting trap surfaces have a superior finishing quality compared to the commonly

Multilayer ion trap technology for scalable quantum computing and quantum simulation 4
used wet etching.

2.2. Multilevel Processing (MLP) Method

In this section a Multilevel Processing (MLP) method is presented, which combines techniques borrowed from MicroElectroMechanical Systems (MEMS) and Integrated Circuits (IC) processing. The method is also compatible with other common substrates used for ion trap technology such as silicon, sapphire, borosilicate glass and quartz.

To demonstrate the simplicity and robustness of our method we have fabricated an ion trap with integrated (3-D) three-dimensional microwave circuitry. It comprises a lower interconnect level L_1 and an upper electrode level L_2 . An additional vertical interconnect access V_1 , called via, allows microwave signals to be transmitted between levels. A more detailed description of the microwave and quantum logic aspects of the trap design and the corresponding characterization will be covered elsewhere [22].

The method presented here mainly consists of six processing steps: (a) wafer preparation, (b) metallization of lower level L_1 , (c) metallization of via V_1 , (d) removal of seed layer, (e) deposition and planarization of dielectric layer D_1 and (f) metallization of upper level L_2 . A schematics of the fabrication flow is given in Fig. 2.

The supporting material is a 3-inch silicon wafer with high resistivity ($\sigma > 1 \times 10^4 \Omega \text{ cm}$). On top of it and as shown in Fig. 2(a), a 2- μm -thick film of Si_3N_4 is deposited by physical enhanced chemical vapor deposition (PECVD). This dielectric film may improve trap operation by avoiding detrimental diffusion of Au into silicon and increasing the flashover voltage as demonstrated in Ref. [23]. Thereafter, a 10-nm-thin layer of Ti and a 50-nm-thin layer of Au are thermally evaporated on top of Si_3N_4 .

To build the lower level L_1 on top of $\text{Si}_3\text{N}_4/\text{Si}$, a negative resist is spin coated and patterned via UV lithography. Once the negative resist is developed to form a resist mold, gold electrodes are grown by electroplating as depicted in Fig. 2(b). After electroplating is completed, the resist mask is stripped and the wafer cleaned under plasma etching.

For the metallization of the via V_1 we repeat the photolithography and electroplating steps presented in (b) but this time on top of L_1 by using a thick ($> 12 \mu\text{m}$) developed negative resist as a plating mold. Electroplated vias on top of L_1 are depicted in Fig. 2(c) after stripping the negative resist mask and plasma cleaning of the wafer.

To remove the Au seed layer and the Ti adhesion layer we use the last dry etching step from the SLP method. This step allows a controllable etch of Au and Ti of 50 nm min^{-1} and 10 nm min^{-1} respectively, resulting in a minimal change of the surface quality on top of both L_1 and V_1 surfaces. The electrically isolated elements on V_1 and L_1 are schematically illustrated in Fig. 2(d).

A dielectric layer is then spin coated on top of L_1 and V_1 and thermally cured (Fig. 2(e)). After thermal curing, excess material is present on top of the underlying structures in L_1 and V_1 . The imprinted dielectric topography is globally planarized

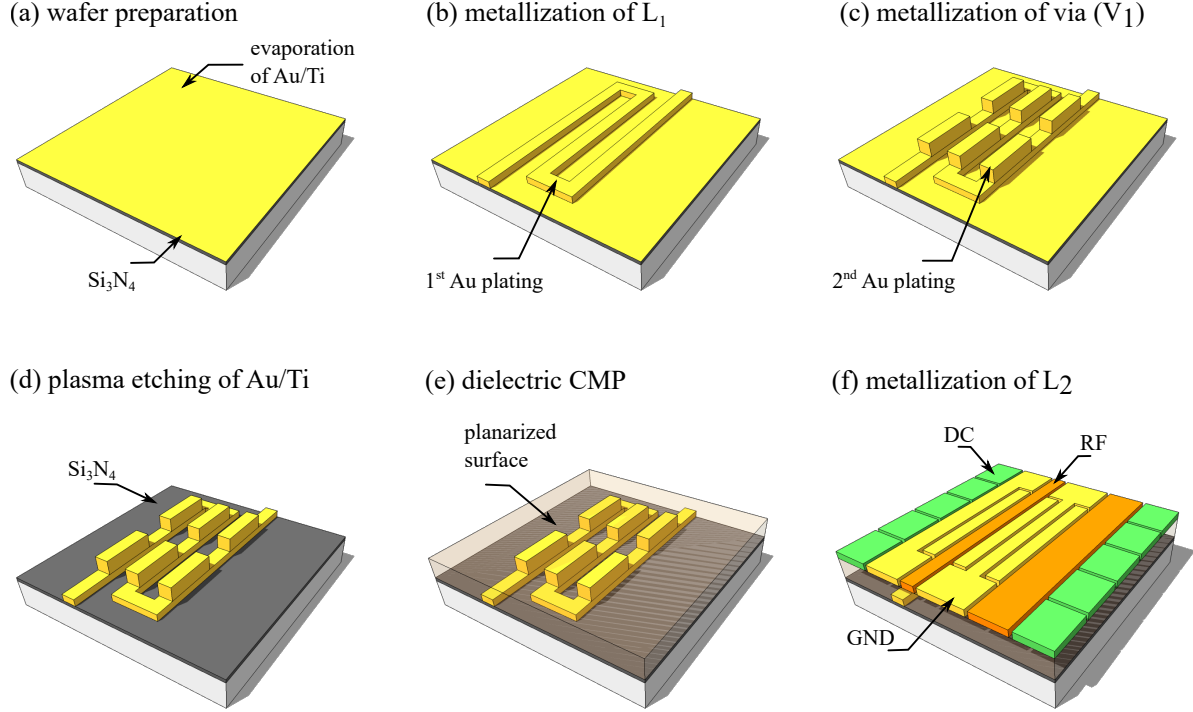


Figure 2. Schematics of the multilevel processing flow. (a) A wafer is coated with a conductive Au/Ti bilayer film. (b) A lower level (L_1) is formed via electroplating. (c) a via V_1 is electroplated on top of L_1 . (d) Dry etching of Au/Ti bilayer film. (e) A polymer is spin coated over both L_1 and V_1 and subsequently planarized by CMP. (f) A second metallization L_2 repeating steps (a), (b) and (d) on a planarized dielectric surface. Exposed dielectric between electrodes in L_2 is removed by plasma etching down to the top surface of the Si_3N_4 layer.

through a chemical-mechanical polishing (CMP) step, which is stopped at the top of V_1 or close to it. To assure electrical contact between V_1 and the subsequent level L_2 a local etch-back process is performed.

To define the top metal layer the SLP method is again employed but this time on top of the planarized polymer surface (Fig. 2(f)). Once the plating has been completed and the resist mold removed, the remaining polymer film between gaps underneath L_2 is etched down to the Si_3N_4 layer by a fluorine-based plasma to hide possible patch potentials built on the exposed insulator.

3. Fabrication outcome and trap operation

Here we briefly present the design and characterization of a trap with 3-D microwave conductors integrated into a microfabricated ion trap using the MLP method. The microwave circuitry is embedded to implement quantum logic operations using near-field microwaves [24, 13, 25, 26]. The specific design is discussed elsewhere in detail [?] and here only described as one of many scenarios that benefits from the multilayer technology.

In the upper level (L_2) the trap includes two RF electrodes and ten DC electrodes to confine the ions to a local minimum (x_0, z_0) , see Fig. 3(a). A microwave signal (white arrows) of frequency 1 GHz can be applied on a 3-D microwave meander (MWM) conductor between two contact points labeled as “F” and “G”, thus generating an oscillating magnetic near-field gradient B' in the xz -radial plane with a local minimum at (x_1, z_1) . The three apparent independent microwave conductors indicated by the white arrows are indeed part of a single 3-D microwave meander connected to L_1 by vias and routed over L_1 as indicated in Fig. 3. A central part of a diced trap chip ($5\text{ mm} \times 5\text{ mm}$) fabricated using the MLP method is presented in Fig. 3(a). There are also two additional microwave conductors (MWC) surrounding the central DC electrodes, in which an oscillating current (black arrows) can be applied to produce an oscillating B field.

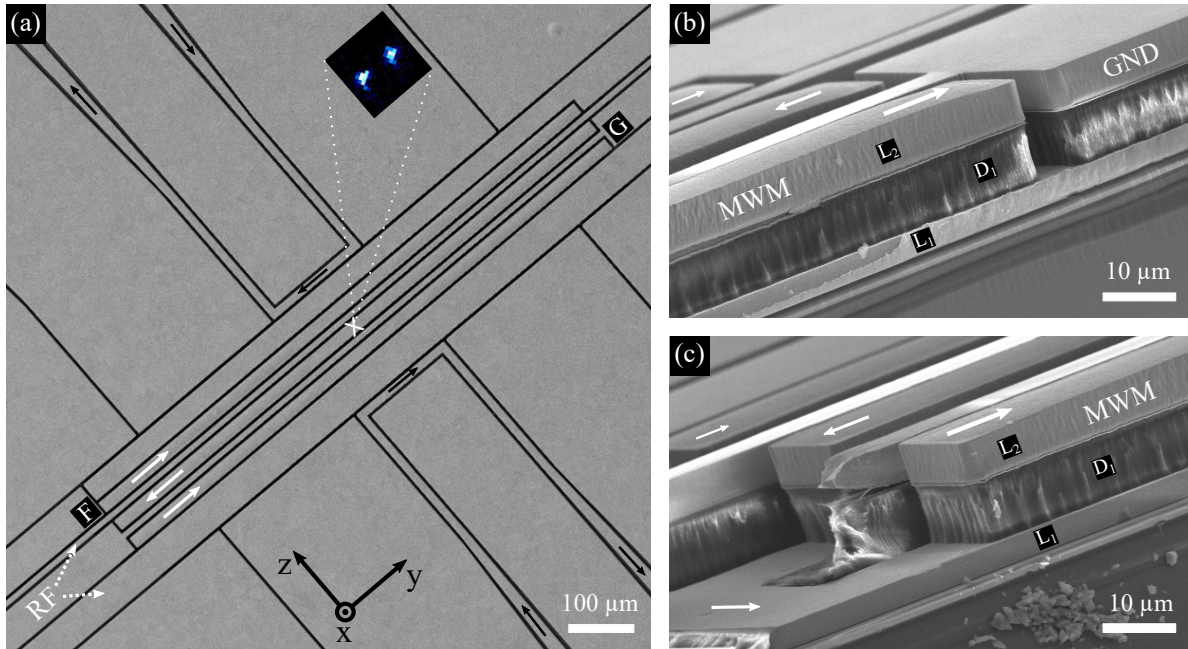


Figure 3. SEM micrograph of the central part of a trap chip fabricated using the MLP method. White and black arrows are drawn on top of the microwave conductors as a guide for the eye. (a) upper metal level L_2 of the trap chip in which black lines correspond to electrode gaps of about $5\text{ }\mu\text{m}$. Ions are trapped at $d = 35\text{ }\mu\text{m}$ above the position marked as “X”. (b) Part of a cleaved chip showing a cross section mainly on the xy -plane around position “G”. (c) Similar to (b) but with a close-up corresponding to position “F” in (a).

A cleaved chip revealing a cross-section view of the metal-dielectric stack around position “F” position “G” is shown in Fig. 3(b) and Fig. 3(c)), respectively. The ion trap (RF and DC electrodes) as well as the uppermost part of the MWM conductor are entirely located in L_2 , whereas the microwave signals and the ground plane are routed between L_1 and L_2 through vias in V_1 (not visible in the micrograph but behind D_1 in Fig. 3(b) and (c)).

Removing both Au and Ti films by means of dry etching has improved the

trap surface quality. For a similar chip as the one here presented an rms roughness $R_{rms} = 8.3(5)$ nm is obtained by atomic-force microscopy over an area of $25 \mu\text{m} \times 25 \mu\text{m}$. This represents a two-order of magnitude improvement when compared to a wet etching process using aqua regia [27]. These nearly mirror-like surfaces are relevant since there is a reduction of stray light scattered in the direction perpendicular to the trap surface during resonance fluorescence imaging for ion state detection. Also an ion trap with minimal surface roughness might be less prone to anomalous motional heating at cryogenic temperatures [28].

The diced trap chip is glued onto a copper block and wirebonded to a custom printed circuit board for filtering and signal routing. The whole assembly is installed in a vacuum system at a pressure better than 1×10^{-11} mbar and connected to an in-vacuum coaxial resonator similar to the one used in Ref. [29]. For ion loading we employ a laser ablation scheme [27] and subsequent two-photon ionization using 235 nm light [30]. Single ${}^9\text{Be}^+$ ions are loaded at $35 \mu\text{m}$ above the upper surface of L_2 around the position “X” (see Fig. 3(a)).

We supply to the trap an RF drive frequency of $\Omega_{RF} = 2\pi \times 176.5$ MHz with amplitude $V_{RF} = 100$ V and DC voltages ranging within ± 25 V. To determine the trap frequencies we apply an oscillating tickle voltage to one of the DC electrodes and scan the frequency [31]. Once the tickle drive is resonant with a secular frequency, the motion of the ion is excited and the ion fluorescence drops (Fig. 4(a)). We measure secular trap frequencies of $(\omega_y, \omega_{LF}, \omega_{HF}) = 2\pi \cdot (4.02, 5.23, 8.59)$ MHz, where the high-frequency (HF) and low-frequency (LF) radial modes form an angle of -5.9° relative to the x -axis and z -axis, respectively.

Finally we employ the integrated microwave conductors to manipulate the internal state of the ion. Fig. 4(b) shows Rabi oscillations on the qubit transition $|F = 2, m_F = +1\rangle \rightarrow |F = 1, m_F = +1\rangle$ [27] of the electronic ground state ${}^2S_{1/2}$ of a single ${}^9\text{Be}^+$ ion at an external magnetic field of $|\mathbf{B}_0| = 22.3$ mT when applying a microwave current of frequency $\omega_0 \simeq 1082.55$ MHz to one of the MWC conductors. Here, F is referring to the total angular momentum \mathbf{F} and m_F the quantum number of its projection on \mathbf{B}_0 . The state readout is carried out via ion fluorescence detection on the closed-cycling transition $|S_{1/2}, F = 2, m_F = 2\rangle \rightarrow |P_{3/2}, m_J = +3/2, m_I = +3/2\rangle$, combined with suitable microwave transfer pulses [27].

4. Conclusion and Outlook

We have presented a novel multilayer method for fabricating scalable surface-electrode ion traps. The flexibility and robustness of the method allows to benchmark the integration of 3-D microwave circuitry into a multilayer ion trap. Furthermore, we have demonstrated successful trapping of ${}^9\text{Be}^+$ and basic qubit manipulation by applying microwave oscillating currents on one of the conductors.

The MLP method presented here can in principle be extended to a nearly arbitrary number of layers to comply with the stringent needs of scaling surface-electrode ion traps.

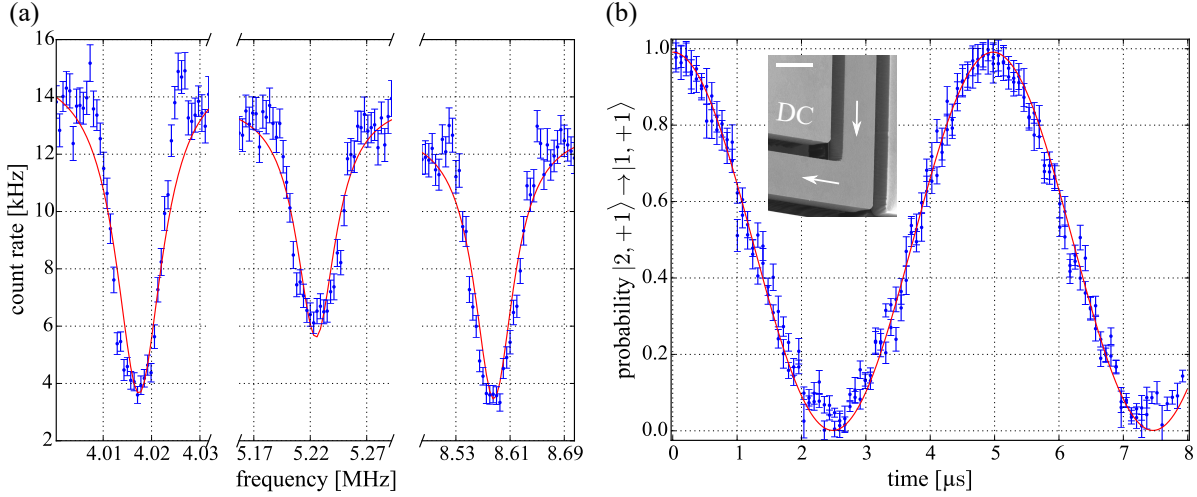


Figure 4. Secular frequencies and microwave qubit transition. (a) Motional frequency measurements using the DC tickle method. The (red) solid lines show Lorentzian fits to the data. The left axis corresponds to the photon average counts after a fluorescence detection of 1.3 ms. (b) Rabi flopping on the qubit transition using a microwave conductor embedded in the trap surrounding a central DC electrode (inset). The white scale bar corresponds to 10 μm and arrows are used only as a guide for the eye.

Moreover, the method permits the integration of three-dimensional and planarized features with high aspect ratio. This technique opens new routes towards the realization of more complex and powerful ion trap devices.

In contrast to a typical CMOS situation where the “device” is fabricated on top of the substrate, with interconnect layers on top of the device, in our case the “device” is the top electrode layer which is controlling the ion(s), whereas the layers closer to the substrate are used as interconnects. In the future, these lower interconnects may be combined with through-wafer vias to achieve contacting of the ion trap chip from the backside, eliminating the need of wirebonds and likely obstruction of laser beams. Through-wafer slots for back-side ion loading can also be produced in the same way. These same techniques could be applied to realize so-called analog quantum simulators in ion trap arrays [32, 33, 34], possibly with integrated control [35]. Moreover, such an approach may enable the embedding of complex integrated components such as trench capacitors [36, 37], low-loss integrated waveguides [38]; or the realization of more elaborate devices including reliable ion-transport junctions [39, 40], increased optical access [17] or manipulation of scalable arrays of two-dimensional trapped ion systems [33, 34].

The MLP method can also be used to extend multilayer “atom chips” [21, 41, 42] or to fabricate scalable hybrid atom-ion traps [43, 44] for quantum many-body physics experiments and quantum sensing with neutral atoms. In this context the thick metal conductors can support substantial currents required for magnetic trapping and the planarization together with the demonstrated minimized surface roughness allows the implementation of mirror-like surfaces and transfer coatings for integrated magneto-

optical traps.

Acknowledgements

We acknowledge support by the PTB cleanroom facility team, in particular T. Weimann and P. Hinze. We also acknowledge support by the LNQE cleanroom staff in particular O. Kerker. We acknowledge funding from PTB, QUEST, LUH, NTH (project number 2.2.11) and DFG through CRC 1227 DQ-*mat*, project A01.

References

- [1] Gaebler J, Tan T, Lin Y, Wan Y, Bowler R, Keith A, Glancy S, Coakley K, Knill E, Leibfried D and Wineland D 2016 *Physical Review Letters* **117** 060505 URL <http://link.aps.org/doi/10.1103/PhysRevLett.117.060505>
- [2] Ballance C, Harty T, Linke N, Sepiol M and Lucas D 2016 *Physical Review Letters* **117** 060504 URL <http://link.aps.org/doi/10.1103/PhysRevLett.117.060504>
- [3] Harty T, Sepiol M, Allcock D, Ballance C, Tarlton J and Lucas D 2016 *Physical Review Letters* **117** 140501 URL <http://link.aps.org/doi/10.1103/PhysRevLett.117.140501>
- [4] Weidt S, Randall J, Webster S, Lake K, Webb A, Cohen I, Navickas T, Lekitsch B, Retzker A and Hensinger W 2016 *Physical Review Letters* **117** ISSN 0031-9007, 1079-7114 URL <https://link.aps.org/doi/10.1103/PhysRevLett.117.220501>
- [5] Monroe C and Kim J 2013 *Science* **339** 1164–1169 ISSN 0036-8075, 1095-9203 URL <http://science.sciencemag.org/content/339/6124/1164>
- [6] Seidelin S, Chiaverini J, Reichle R, Bollinger J J, Leibfried D, Britton J, Wesenberg J H, Blakestad R B, Epstein R J, Hume D B, Itano W M, Jost J D, Langer C, Ozeri R, Shiga N and Wineland D J 2006 *Physical Review Letters* **96** 253003 URL <http://link.aps.org/doi/10.1103/PhysRevLett.96.253003>
- [7] Wineland D J, Monroe C R, Itano W M, Leibfried D, King B E and Meekhof D M 1998 *J. Res. NIST* **103** 259–328 URL <http://nvl.nist.gov/pub/nistpubs/jres/103/3/j33win.pdf>
- [8] Kielpinski D, Monroe C and Wineland D J 2002 *Nature* **417** 709–711 ISSN 0028-0836 URL <http://dx.doi.org/10.1038/nature00784>
- [9] Lekitsch B, Weidt S, Fowler A G, Mølmer K, Devitt S J, Wunderlich C and Hensinger W K 2017 *Science Advances* **3** e1601540 ISSN 2375-2548 URL <http://advances.sciencemag.org/content/3/2/e1601540>
- [10] Hughes M D, Lekitsch B, Broersma J A and Hensinger W K 2011 *Contemporary Physics* 1–25 ISSN 0010-7514, 1366-5812 URL <http://www.tandfonline.com/doi/abs/10.1080/00107514.2011.601918>
- [11] Merrill J T, Volin C, Landgren D, Amini J M, Wright K, Doret S C, C-S Pai, Hayden H, Killian T, Faircloth D, Brown K R, Harter A W and Slusher R E 2011 *New Journal of Physics* **13** 103005 ISSN 1367-2630 URL <http://stacks.iop.org/1367-2630/13/i=10/a=103005>
- [12] Mehta K K, Bruzewicz C D, McConnell R, Ram R J, Sage J M and Chiaverini J 2016 *Nature Nanotechnology* **11** 1066–1070 ISSN 1748-3387 URL <http://www.nature.com/nnano/journal/v11/n12/full/nnano.2016.139.html>
- [13] Ospelkaus C, Warring U, Colombe Y, Brown K R, Amini J M, Leibfried D and Wineland D J 2011 *Nature* **476** 181–184 ISSN 0028-0836 URL <http://dx.doi.org/10.1038/nature10290>
- [14] Cho D I D, Hong S, Lee M and Kim T 2015 *Micro and Nano Systems Letters* **3** 1 ISSN 2213-9621 URL <http://mns1-journal.springeropen.com/articles/10.1186/s40486-015-0013-3>
- [15] Hong S, Lee M, Cheon H, Kim T and Cho D I D 2016 *Sensors* **16** 616 URL <http://www.mdpi.com/1424-8220/16/5/616>

- [16] Stick D, Fortier K M, Haltli R, Highstrete C, Moehring D L, Tigges C and Blain M G 2010 *1008.0990* URL <http://arxiv.org/abs/1008.0990>
- [17] Maunz P L W 2016 High Optical Access Trap 2.0. Tech. Rep. SAND-2016-0796R Sandia National Lab. (SNL-NM), Albuquerque, NM (United States) URL <https://www.osti.gov/biblio/1237003-high-optical-access-trap>
- [18] Schmied R 2010 *New Journal of Physics* **12** 023038 ISSN 1367-2630 URL <http://iopscience.iop.org/1367-2630/12/2/023038>
- [19] Timoney N, Baumgart I, Johanning M, Varon A F, Plenio M B, Retzker A and Wunderlich C 2011 *Nature* **476** 185–188 ISSN 0028-0836 URL <http://dx.doi.org/10.1038/nature10319>
- [20] Treutlein P 2008 *Coherent manipulation of ultracold atoms on atom chips* Ph.D. thesis Ludwig-Maximilians-Universität München
- [21] Fortágh J and Zimmermann C 2007 *Reviews of Modern Physics* **79** 235 URL <http://link.aps.org/doi/10.1103/RevModPhys.79.235>
- [22] Hahn H, Zarantonello G, Bautista-Salvador A, Kohnen M, Wahnschaffe M, Ospelkaus C and Schoebel J *in preparation*
- [23] Sterling R C, Hughes M D, Mellor C J and Hensinger W K 2013 *Applied Physics Letters* URL <http://aip.scitation.org/doi/10.1063/1.4824012>
- [24] Ospelkaus C, Langer C E, Amini J M, Brown K R, Leibfried D and Wineland D J 2008 *Physical Review Letters* **101** 090502 URL <http://link.aps.org/doi/10.1103/PhysRevLett.101.090502>
- [25] Warring U, Ospelkaus C, Colombe Y, Brown K R, Amini J M, Carsjens M, Leibfried D and Wineland D J 2013 *Physical Review A* **87** 013437 URL <http://link.aps.org/doi/10.1103/PhysRevA.87.013437>
- [26] Carsjens M, Kohnen M, Dubielzig T and Ospelkaus C 2014 *Applied Physics B* **114** 243–250 ISSN 0946-2171, 1432-0649 URL <http://link.springer.com/article/10.1007/s00340-013-5689-6>
- [27] Wahnschaffe M, Hahn H, Zarantonello G, Dubielzig T, Grondkowski S, Bautista-Salvador A, Kohnen M and Ospelkaus C 2017 *Applied Physics Letters* **110** 034103 ISSN 0003-6951 URL <http://aip.scitation.org/doi/full/10.1063/1.4974736>
- [28] Lin K Y, Low G H and Chuang I L 2016 *Physical Review A* **94** 013418 URL <https://link.aps.org/doi/10.1103/PhysRevA.94.013418>
- [29] Jefferts S R, Monroe C, Bell E W and Wineland D J 1995 *Physical Review A* **51** 3112 URL <http://link.aps.org/doi/10.1103/PhysRevA.51.3112>
- [30] Leibbrandt D R, Clark R J, Labaziewicz J, Antohi P, Bakr W, Brown K R and Chuang I L 2007 *Physical Review A* **76** 055403 URL <http://link.aps.org/doi/10.1103/PhysRevA.76.055403>
- [31] Home J P, Hanneke D, Jost J D, Leibfried D and Wineland D J 2011 *New Journal of Physics* **13** 073026 ISSN 1367-2630 URL <http://stacks.iop.org/1367-2630/13/i=7/a=073026>
- [32] Porras D and Cirac J I 2004 *Physical Review Letters* **92** 207901 URL <http://link.aps.org/doi/10.1103/PhysRevLett.92.207901>
- [33] Mielenz M, Kalis H, Wittemer M, Hakelberg F, Warring U, Schmied R, Blain M, Maunz P, Moehring D L, Leibfried D and Schaetz T 2016 *Nature Communications* **7** ncomms11839 ISSN 2041-1723 URL <https://www.nature.com/articles/ncomms11839>
- [34] Bruzewicz C D, McConnell R, Chiaverini J and Sage J M 2016 *Nature Communications* **7** ISSN 2041-1723 URL <http://www.nature.com/articles/ncomms13005>
- [35] Chiaverini J and Lybarger W E 2008 *Physical Review A* **77** 022324 URL <http://link.aps.org/doi/10.1103/PhysRevA.77.022324>
- [36] Allcock D T C, Harty T P, Janacek H A, Linke N M, Ballance C J, Steane A M, Lucas D M, Jarecki R L, Habermehl S D, Blain M G, Stick D and Moehring D L 2012 *Applied Physics B* **107** 913–919 ISSN 0946-2171, 1432-0649 URL <http://link.springer.com/article/10.1007/s00340-011-4788-5>
- [37] Guise N D, Fallek S D, Stevens K E, Brown K R, Volin C, Harter A W, Amini J M, Higashi R E,

- Lu S T, Chanhvongsak H M, Nguyen T A, Marcus M S, Ohnstein T R and Youngner D W 2015 *Journal of Applied Physics* **117** 174901 ISSN 0021-8979 URL <https://aip.scitation.org/doi/10.1063/1.4917385>
- [38] West G N, Loh W, Kharas D, Sorace-Agaskar C, Mehta K K, Sage J, Chiaverini J and Ram R J 2018 *arXiv:1808.00429 [physics]* ArXiv: 1808.00429 URL <http://arxiv.org/abs/1808.00429>
- [39] Moehring D L, Highstrete C, Stick D, Fortier K M, Haltli R, Tigges C and Blain M G 2011 *New Journal of Physics* **13** 075018 ISSN 1367-2630 URL <http://stacks.iop.org/1367-2630/13/i=7/a=075018>
- [40] Wright K, Amini J M, Faircloth D L, Volin C, Doret S C, Hayden H, C-S Pai, Landgren D W, Denison D, Killian T, Slusher R E and Harter A W 2013 *New Journal of Physics* **15** 033004 ISSN 1367-2630 URL <http://stacks.iop.org/1367-2630/15/i=3/a=033004>
- [41] Trinker M, Groth S, Haslinger S, Manz S, Betz T, Schneider S, Bar-Joseph I, Schumm T and Schmiedmayer J 2008 *Applied Physics Letters* **92** 254102 ISSN 0003-6951 URL <http://aip.scitation.org/doi/full/10.1063/1.2945893>
- [42] Bohi P, Riedel M F, Hoffrogge J, Reichel J, Hansch T W and Treutlein P 2009 *Nature Physics* **5** 592-597 ISSN 1745-2473 URL <http://dx.doi.org/10.1038/nphys1329>
- [43] Härter A and Denschlag J H 2014 *Contemporary Physics* **55** 33-45 ISSN 0010-7514 URL <https://doi.org/10.1080/00107514.2013.854618>
- [44] Bahrami A, Müller M, Drechsler M, Joger J, Gerritsma R and Schmidt-Kaler F 2018 *arXiv:1811.07670 [physics, physics:quant-ph]* ArXiv: 1811.07670 URL <http://arxiv.org/abs/1811.07670>